

PREDICTION OF SURFACE MOTIONS
DURING THE EXPLOITATION OF THE SHAFT
PILLAR IN THE COAL MINE MAYRAU

MILOŠ VENCOVSKÝ

Institute of Rock Structure and Mechanics, Academy of Sciences of Czech Republic
V Holešovičkách 41, 182 09 Prague, Czech Republic

ABSTRACT. The Institute of Rock Structure and Mechanics (IRSM) started, in 1992, the investigation of consequences of coal exploitation within the shaft pillar of the mine Mayrau (Kladno coal district) on the origination of induced seismic and deformation phenomena in the overlying rock massif. A part of this research became also the prediction of phenomena occurring at the surface in consequence of undermining. These prognoses were obtained in two ways: by computing and by physical methods. Computer prognoses issued from the actual knowledge of the theory of undermining and the author developed, for their realization, his original software. Physical prognoses were based on the measurement of geometrical deformations of the surface of a physical model constructed from equivalent materials, in which exploitation of the shaft pillar was simulated. Special attention has been paid to the comparison of results of both of these prognostical methods and their effectiveness in the research of undermining.

1. INTRODUCTION

The investigation of the problem was started in 1992 to the order of the mine Mayrau with the aim to study the effect of coal exploitation within the shaft pillar on the origination of induced seismic phenomena and occurrence of deformation phenomena within the overlying rock mass and, eventually, derive the causal nexus between these phenomena and occurrence of rock bursts. Later, this problem has been incorporated as an independent theme into the scientific grant of the Czech republic, studied in IRSM since the year 1993 till present time.

Mayrau is one from two mines of the Kladno coal district, where the coal exploitation just enters the hitherto intact coal reserves within the shaft pillar. Problems of surface manifestations of this exploitation become therefore highly actual. This is connected not only with the necessity of protection of the shaft and surface structures in the mine's neighbourhood, but also with purely methodical reasons, since a similar exploitation has been started recently in another mine in the district without preliminary research works of the kind. Results of the undermining problems of the shaft Mayrau may therefore be effectively used also for this second mine of the Kladno district. Of course, they may also present a valuable contribution to

the knowledge basis within the theory of undermining, which is studied to our day both in our country and abroad.

The concept of the overall solution of the problem was based on the confrontation of two entirely different methods of prediction of motion manifestations of the overlying rock mass for several development stages from beginning of exploitation in 1993 till its planned ending in the year 2000. The matter concerned prognoses obtained, on the other hand, by means of physical modelling and, on the other hand, those derived on the basis of automatized computation issuing from the theory of undermining, developed since the beginning of this century, namely in Germany and Poland [Neset 1984; Neubert 1958].

The method of physical derivation of these prognoses on the basis of simulated excavation within the shaft pillar prepared from equivalent model material of the overlying strata series will not be described in detail in this contribution, because the topic is treated in another publication [Skořepová, Filip 1994]. Nevertheless, for further reasoning and formulation of final results, some data, notions and characteristics, concerning this model solution, should be mentioned, though. As already said, the matter was of an equivalent model of spatial type, simulating the original rock mass vertically within the extent of the whole overburden, and horizontally within the sufficiently wide neighbourhood of the shaft pillar. The model scale was 1:750. The model simulation of the original rock mass has been carried out considering all available geologico-geotechnical information, with approximately fulfilling the important initial assumption that the critical angle of effects would attain the value of about 65° , which characterizes very well the effect of undermining within the Kladno district [Lucák 1969; Kadanka 1937]. The scope of the model experiment was the assessment of motion phenomena, which take place on the model surface during various phases of mining. These phenomena were measured by the analytical stereophotogrammetric method, formulated and elaborated by the author the final software [Vencovský 1992], and which enabled the spatial displacement of survey points, chosen at the model surface in sufficient quantity, to be measured precisely. Results of these measurements were then processed into such a final hardcopy form, which enabled the qualitative and quantitative graphic confrontation of these results with results of computer-based prognoses. The author's own software, prepared earlier [Vencovský 1989] and intended for graphical illustration of so-called digital raster models of non-analytical surfaces in the form of contour plans, coloured hypsometric plans and so-called three-dimensional views, was an effective tool for the acquirement of these documents.

Computer prognoses, issuing from long-lasting mine surveying experience and information as well from known theories of undermining effects, were based on another author's software, specially developed to this purpose.

The problem of formulation of prognoses of this type have been, up to now, a topic of vivid interest of experts, not only on the nation scale, though the first local functional softwares are dated from the end of sixtieths [Havlík 1967; Hradil 1969]. Among the actual commercially offered products, the program POKLESY OL, developed by IMGE [Čimbura, Hynčicová 1994] and the program developed in the Mining Survey Base of VŠB in Ostrava and described in [Murysová, Vočyán 1994],

should be quotes. Both of these program systems are theoretically based on the principle of formation of a subsidence basin according to Knothe [Neset 1984] and, as far as the numerical computing is concerned, on the application of the so-called triangular method, described by Hradil in the already quoted article [Hradil 1969]. The development of an entirely independent software by the author at the time, when both above-quoted programs have already been available, was motivated by following reasons.

The universal application of the so-called effect function (see below), introduced by Knothe, must not always meet with the best results, because the analytical form of this function should correspond to the mechano-physical behaviour of the strained rock mass, which, of course, can be quite different in different mine district. It is therefore well-founded to look for optimum subsidence forecast on the basis of numerical experiments, consisting in the use of various, even considerably complicated forms on the effect function. The mentioned triangular method, which enables the resulting subsidence in a certain point of the undermined surface to be calculated on the basis of numerical determination of the value of double integral above the region with a very complex border, is based on the assumption that an indefinite integral of the effect function can be found, which is always fulfilled for the Knothe's effect function or functions introduced also by others experts. The completely general choice of the effect function requires a new method to be formulated, which would retain the above-mentioned purpose of the triangular method.

The author therefore did not use, for mentioned reasons, the already known software products [Čimbura, Hynčicová 1994; Murysová, Vochyán 1994], because he did not attempt to prepare the subsidence prognoses for the needs of just this single mine, but to compare various modifications of these prognoses with physical ones and to derive general information on their suitability, effectiveness and usefulness. The subsequent chapter should therefore be understood within the mentioned author's struggle and some of the here mentioned and generally known information be taken as members of a robust deductive reasoning required for the deduction of an algorithm and for programmer-related expression of the author's intention.

2. BASIC THEORETICAL ASSUMPTIONS AND INFORMATION

Most of the mine-survey hypotheses and theories of surface motions of the terrain relief, due to the exploitation of economic minerals in horizontally deposited seams or caused by underground works of a similar excavation character, are issuing from several basic assumptions (Fig. 1).

1. The differentially exploited volume dq in the point $Q(X, Y, h)$ of a seam with thickness m , horizontally deposited in the depth h will cause that the surface point $P(\xi, \eta, 0)$ will be shifted, by the differential displacement dp , whose direction lies in the connecting line PQ and whose value is proportional to the function of length of the line segment $\kappa = \overline{PQ}$.

$$dp = \kappa \cdot s(q) \cdot dq \quad (1)$$

For the mentioned assumption of the horizontal deposition of the seam, i.e. for $h = \text{const.}$ and for a sufficiently small seam thickness, compared to its deposition

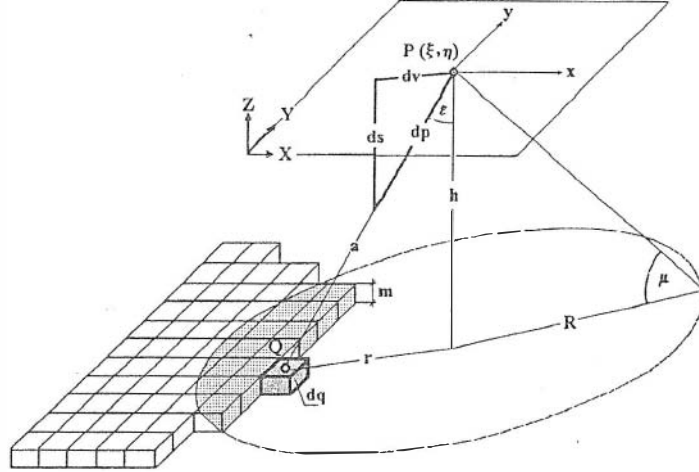


FIG. 1 Effect of differential excavation on the displacement of the point P

depth, it will hold, within the system of polar coordinates,

$$dp = \kappa \cdot m \cdot r \cdot u(r) \, d\varphi \, dr, \quad (2)$$

and in cartesian system of coordinates

$$dp = \kappa \cdot m \cdot f(x, y) \, dx \, dy, \quad (3)$$

when

$$a = \sqrt{h^2 + r^2} = \sqrt{h^2 + x^2 + y^2}, \quad (4)$$

and

$$\begin{aligned} x &= X - \xi, \\ y &= Y - \eta. \end{aligned} \quad (5)$$

According to quoted formulation, the function $z = f(x, y)$ represents rotational surface with the rotational axis in the axis z , the curve $z = u(r)$ being the main meridian of this surface.

2. The effect of the differential excavation equals zero at those surface points, where the connecting lines \overline{PQ} include, with horizontal plane, the angle of $\pi/2 - \varepsilon$, wider than the so-called critical angle μ .

3. The resulting displacement p of a certain surface point P is proportional to the sum of all differential displacement vectors, caused by all differential excavations, which can effect the motion of the point P in the sense of the assumption 2. These excavations are forming, summarily, the so-called effective exploited region Ω . When the differential displacement will be considered according to equations (2) or (3), it will hold

$$p = \kappa \cdot m \iint_{\Omega} r \cdot u(r) \, dr \, d\varphi, \quad (6)$$

or

$$p = \kappa.m \iint_{\Omega} f(x, y) dx dy. \quad (7)$$

4. The mentioned formulation of the resulting displacement of a certain point P is still considered irrespective of the inseparable time dependence between the successive progress of mining in the effective area and retarding effects of partial displacements of this point. The final and unalterable displacement of the point will be attained with a certain time delay $t = t_m$ after beginning of exploitation within the effective area, when $t = 0$. Incorporation of the effect of time into the above quoted definitions is based on the assumption that a certain momentary displacement $p(t)$ equals to the product of the value of final displacement p and the value of "time factor", which is the value of a certain empirically derived time function $z(t)$. Thus

$$p(t) = p.z(t), \quad (8)$$

where

$$z(0) = 0, \quad z(t_m) = 1.$$

These four basic assumptions result into the derivation of further information of hypothetic character, which helps form an integrated theoretical basis of knowledge and effectively assists in the further solution of problems associated with undermining.

Subsidence s of the point P will be defined as vertical component of the resulting vector of displacement p of this point. If the resulting vector \vec{p} includes, with the horizontal plane, the angle ε , then

$$s = p. \cos \varepsilon. \quad (9)$$

Horizontal displacement v of the point P is defined as horizontal component of resulting displacement vector

$$v = p. \sin \varepsilon. \quad (10)$$

The horizontal displacement is usually resolved into components v_x and v_y , which are parallel with axes of the relative horizontal coordinate system X, Y .

Full effective area appertaining to a certain surface point P is the area Φ of the base of the right circular cone with height h and the apex in this point, whose surface lines include, with the horizontal plane, the angle of $\pi/2 - \mu$. Thus, the radius R of the full effective area is

$$R = h. \cotg \mu. \quad (11)$$

Maximum subsidence s_{max} is the subsidence of a certain point P for the case that the effective mined-out area appertaining to it lies within the extent of the full effective area $\Omega = \Phi$ and that the value of the time function equals 1. Under

these circumstances, the maximum subsidence is, at the same time, also the maximum displacement and can therefore be defined, with regard to generally known information, as

$$s_{\max} = m.a, \quad (12)$$

where a is the so-called coefficient of exploitation, attaining values within $[0, 1]$ and m is the thickness of the horizontally deposited seam.

Considering the equations (6) and (7) and also the already mentioned character of the function $f(x, y)$, it is possible to derive, for s_{\max} , the following relations:

$$s_{\max} = \kappa.m \iint_{\Phi} f(x, y) dx dy = 4\kappa.m \int_0^R dx \int_0^{\sqrt{R^2-x^2}} f(x, y) dy, \quad (13)$$

or

$$s_{\max} = 4\kappa.m \int_0^{\pi/2} d\varphi \int_0^R r.u(r) dr = 2\pi\kappa.m \int_0^R r.u(r) dr \quad (14)$$

and to determine, from them, for both alternatives of coordinate systems, expressions for hitherto unknown coefficients of proportionality κ . Substituting these expressions into equations (6) and (7), with consideration of the relations (8) and (12), the following relation can be derived, for displacement p at a general surface point $P(\xi, \eta)$:

$$p(\xi, \eta) = m.a.z(t) \frac{\iint_{\Omega} f(x, y) dx dy}{4 \int_0^R dx \int_0^{\sqrt{R^2-x^2}} f(x, y) dy}, \quad (15)$$

or

$$p(\xi, \eta) = m.a.z(t) \frac{\iint_{\Omega} r.u(r) dr d\varphi}{2\pi \int_0^R r.u(r) dr}, \quad (16)$$

if the local polar coordinate system is introduced into the point P .

The two entirely equivalent relations become the basis of all following reflections and formulations of procedures for the determination of computer prognoses of motion phenomena of the undermined terrain. It may be added that these relations are usually expressed uniformly in the form of a product of four parameters [Neset 1984]

$$p(\xi, \eta) = m.a.z.e, \quad (17)$$

the significance of individual factors being evident from the comparison of this relation with those mentioned above.

The function $u(r)$ evt. $f(x, y)$ uses to be called "effect function", which was already mentioned in the introduction chapter. The analytical form of this function has been modified, during the development of research of geometry of motion phenomena in the undermined territory, by several, namely German and Polish experts, who consider practical results of subsidence measurements. It should be said that generalized results, which resulted from the analysis of such measurements with regard to the geometry mining, sometimes differed very much, depending on

geological and geotechnical parameters of the overlying rock masses, as well as on the mining and exploitation conditions, specific to individual mine district. Due to efforts to describe, as well as possible, the undermining effects in a certain mine locality and form thus a basis for computing the subsidence prognoses, several “effect functions” have been formulated, the most frequently used being the already mentioned Knothe’s function. Although these functions have got entirely different forms, most of them have the common property that there are even functions, largely of the Gaussian (bell-like) character. For comparative studies with the aim to derive, for the given mine district, a most suitable forms of these functions, the function of the $u(r)$ type is transformed by substitution

$$k = \frac{r}{R}, \quad 0 \leq k \leq 1 \tag{18}$$

into the function $g(k)$ and, similarly, the function of the type $f(x, y)$ by substitution

$$i = \frac{y}{R}, \quad j = \frac{x}{R}, \quad 0 \leq i \leq 1, \quad 0 \leq j \leq 1 \tag{19}$$

into the function $g(i, j)$. Tab. 1 shows the functions of the type $g(k)$, formulated in the past by most prominent experts in the area of undermining effects [Neset 1984; Neubert 1958].

TABLE 1.

Author	$g(k)$	E
1. Bals	$\frac{1}{1 + k^2 \cdot \cotg^2 \mu}$	$\frac{1}{c} - 1$
2. Perz	$\frac{1}{\sqrt{1 + k^2 \cdot \cotg^2 \mu}}$	$\frac{1}{c^2} - 1$
3. Bayer	$(1 - k^2)^2$	$(1 - \sqrt{c}) \cotg^2 \mu$
4. Sahn	$e^{-4 \cdot k^2}$	$-\frac{1}{4} \cotg^2 \mu \cdot \ln(c)$
5. Knothe	$e^{-\pi \cdot k^2}$	$-\frac{1}{\pi} \cotg^2 \mu \cdot \ln(c)$

Graphical illustration of these functions is given in Fig. 2. It is evident, from both the table and figure, that only the function 3 exactly satisfies the second fundamental assumption about zero effect of mining beyond the limits defined by the critical effect angle. Functions 4 and 5, unlike the functions 1 and 2, satisfy this assumption approximately too. It should be added, in this connection, that the non-fulfillment of the quoted assumption does not mean that displacements of the surface points determined according to equations (15) and (16) will not equal zero beyond the mentioned limit. It is evident, from both formulae, that values of surface integrals for points beyond the mentioned limit will equal zero

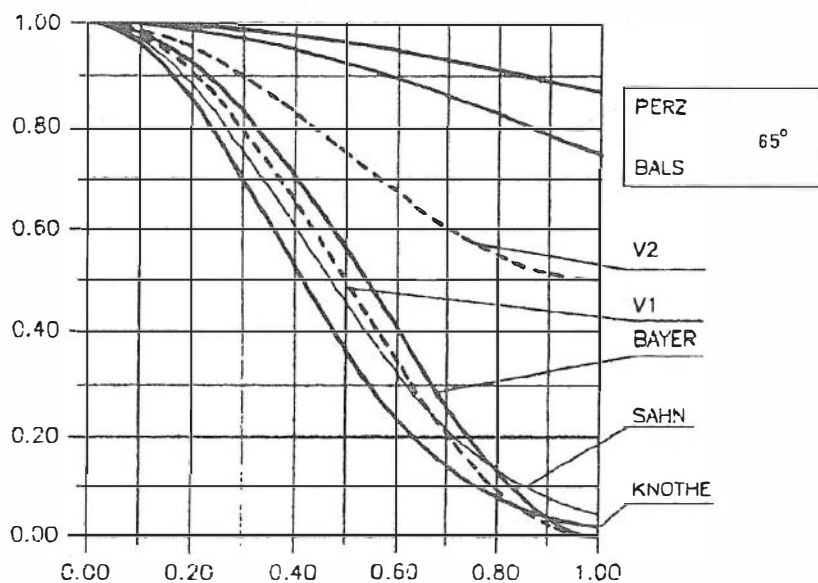


FIG. 2. Graphical illustration of effect function from Table 1.

in numerators, because their integration range is empty set. It is remarkable that just the Bals' method of prognostical computing of undermining effects, has been, until recently, the most used one and proved fairly suitable for the estimation of subsidences in our coal district [Neset 1984; Lucák 1969]. Nevertheless, the theoretical basis of both already discussed available computing methods for the estimation of effects of undermining [Čimbura, Hynčicová 1994; Murysová Vochyán 1994] is formed by the Knothe's function, in spite of the fact that its application has not been supported by a deeper analysis and by comparison of theoretical and real subsidence or motions in undermined territories [Hradil 1969].

3. ANALYTICAL ASSESSMENT OF SURFACE MOTIONS ABOVE WORKED-OUT HORIZONTALLY DEPOSITED SEAMS

Analytical derivation of superficial motion phenomena above stopes of the mentioned type can be carried out only for stopes of the most simple geometrical form. Although it may seem that the significance of these studies is rather theoretical due to the mentioned circumstances, the obtained results can become useful tools for the comparison of theoretical subsidences or motions with real displacements, measured directly above working faces. The literature refers only to the solution by Bayer [Neset 1984], who derived the analytical form of the subsidence curve, which originates in a vertical section, perpendicular to an infinitely long and straight working face in a horizontally deposited seam, for the "effect function" introduced by him (see Tab. 1). Fig. 3 illustrates this derivation method. For the determination of displacement p of the point P with coordinates ξ, η the generalized equation (15) can be used for the given mining method. Considering the substitution (19), then

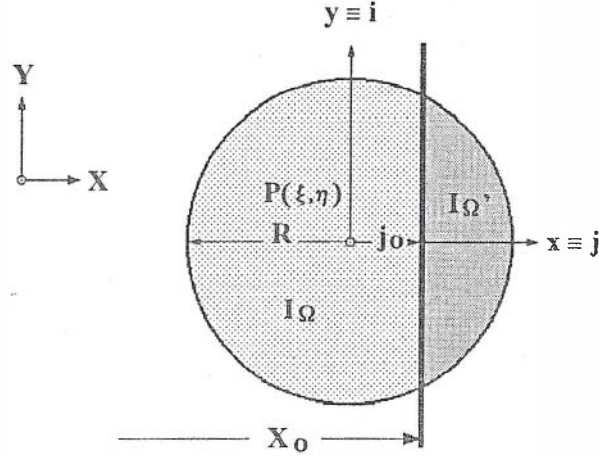


FIG. 3. Diagram for analytical derivation of the subsidence curve above a straight working face.

$$p(\xi, \eta) = s_{\max} \cdot z(t) \frac{I_{\Omega}}{I_{\Phi}} = s_{\max} \cdot z(t) \frac{I_{\Phi} - I_{\Omega'}}{I_{\Phi}}, \quad (20)$$

where

$$I_{\Phi} = 4 \cdot \kappa \cdot m \cdot R^2 \int_0^1 dj \int_0^{\sqrt{1-j^2}} g(i, j) di \quad (21)$$

being the motion effect of working-out the full effective area Φ and

$$I_{\Omega'} = 2 \cdot \kappa \cdot m \cdot R^2 \int_{j_0}^1 dj \int_0^{\sqrt{1-j^2}} g(i, j) di \quad (22)$$

being the motion effect of the unworked part of the full effective area Ω' for a concrete position of the working face $X = X_0$, thus for

$$j_0 = \frac{X_0 - \xi}{R}, \quad (23)$$

when

$$-1 \leq j_0 \leq 1. \quad (24)$$

The equation (20) can be transcribed in the form of

$$p(\xi, \eta) = s_{\max} \cdot z(t) \cdot \left(1 - \frac{1}{2} \frac{\int_{j_0}^1 dj \int_0^{\sqrt{1-j^2}} g(i, j) di}{\int_0^1 dj \int_0^{\sqrt{1-j^2}} g(i, j) di} \right). \quad (25)$$

The quoted equation is the author's generalization of the Bayer's procedure for arbitrarily chosen effect function $g(i, j)$. An analytical solution of the mentioned integrals can, of course, be found, so far as the form of the function $g(i, j)$ allows

it, as it is the above mentioned case, when the concrete wording of the equation (25) can be derived in the form [Neset 1984]

$$p(\xi, \eta) = \frac{s_{\max}}{\pi} z(t) \left(\pi - \arccos(j_0) + j_0 \sqrt{1 - j_0^2 \left(\frac{8}{15} j_0^4 - \frac{26}{15} j_0^2 + \frac{11}{5} \right)} \right). \quad (26)$$

Čechura (in [Neset 1984]) dealt also with the derivation of subsidence curve for the above mentioned type working. Analytical version of its curve can be obtained very simply by means of the equation (25), where the integral (21) will equal the surface of the full effective area Φ and integral (22) will equal the surface of the circle sector Ω' , thus when

$$g(i, j) = \text{const.} \quad (27)$$

Then, the concrete wording of the equation (25) will be

$$p(\xi, \eta) = \frac{s_{\max}}{\pi} z(t) \cdot \left(\pi - \arccos(j_0) + j_0 \sqrt{1 - j_0^2} \right). \quad (28)$$

The quoted equation has a somewhat different form than the original, derived by Čechura. However, it can be transformed into original wording by a simple modification.

Both equations, (26) and (28), define the displacement curves in relation to the initial equation (15). However, Bayer and Čechura derived these equations as equations of subsidence curves. This discrepancy is involved in author's introductory definitions (Chapter 2), which differ, in this connection, somewhat from introductory assumptions of the two quoted authors.

As already stated, preliminary calculations of displacement or subsidences, based on analytical solutions, can be carried out only in exceptional cases. Contemporary requirements put on these calculations are based on the assumption that the geometrical shape of worked faces can be entirely general, thus frequently very complicated, that the worked seam need not be horizontally deposited and that its thickness can vary quite much. Under these circumstances, approximate or purely numerical computing methods, based on computer expression, have to be used. Approximate methods, which enable values of definite integrals in equations (15) and (16) to be found on the basis of known numerico-graphical integration methods, belong already to the past, because they are very elaborate and cumbersome and lead usually to rather inaccurate results.

4. BASIS OF THE AUTHOR'S COMPUTER CALCULATION PROGNOSES OF THE DISPLACEMENT OF UNDERMINED SURFACE

Only a limited quantity of existing experience and information can be found for the formulation of such a basis. In this connection, attention should be paid to two previously mentioned publications [Čimbura, Hynčicová 1994; Murysová, Vochyán 1994], which deal with calculations of this type, but which limit themselves only to the external description of functionality of the software and, as far as the

theoretical principles of numerical integrations in the sense of equations (15) or (16) are concerned, they refer always only to publication [Hradil 1969] and the here described triangular method, which uses the Knothe's effect function. The information background for the preparation of the original software, mentioned in the introductory chapter, was therefore rather limited.

The theoretical basis of this software uses therefore the numerical form of equation (16), into which also the effect of a possible dip of the worked seam was incorporated. The basis of the numerical integrations in this equation is the division of the affected planar surface territory into a network of nodal points of rectangular raster. If the side length of the elementary rectangle is denoted by Δ , the worked seam of the thickness m will be divided into the total number q of finitely small elementary workings (EW) with the volume of $m \cdot \Delta^2$. Each of these EW can be situated in a different depth h_r due to the seam dip. Let me presume, for simplification of this reasoning, that the critical angle of effect μ does not change with the seam dip, which is somewhat contradictory to actual theories. We assume therefore that a certain r -th EW will affect the surface within the extent of a circle with radius

$$R_r = h_r \cdot \cotg \mu . \tag{29}$$

The elementary displacement Δp of nodal point of the raster $P(\xi, \eta)$ due to working out r -th EW at the depth of h_r and whose centre has horizontal coordinates x_r, y_r , defined within the local coordinate system with origin in the point P (Fig. 4) can be, according to (3), approximately defined by the relation

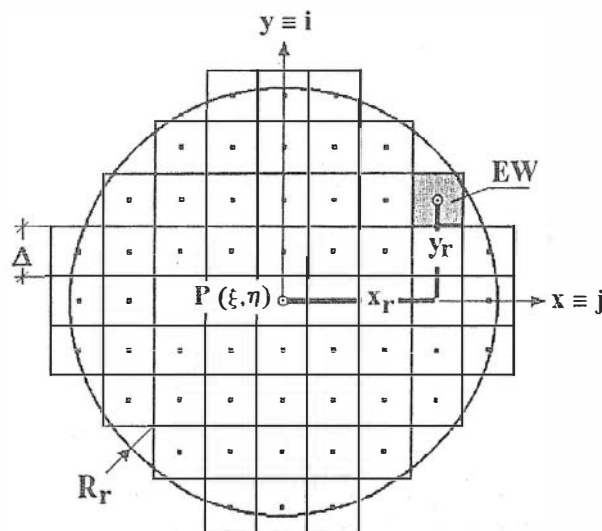


FIG. 4. Position relations between elementary working and the nodal point of the rectangular network.

$$\Delta p = \kappa \cdot m \cdot \Delta^2 f(x_r, y_r) = \kappa \cdot m \cdot \Delta^2 f(j \cdot \Delta, i \cdot \Delta), \tag{30}$$

where j is the linear and i the column-related position index of the centre EW within the rectangular network. The origin of indexing is in point P and it changes toward both positive and negative values. The relation (30) can further be simplified with regard to the already known fact that the function $g(i, j)$ represents the surface of revolution with the main meridian $g(k)$. Therefore

$$\Delta p = \kappa.m.\Delta^2 g(k_r), \quad 0 \leq k_r \leq 1, \quad (31)$$

when

$$k_r = \frac{\sqrt{x_r^2 + y_r^2}}{R_r} = \frac{\sqrt{j^2 + i^2}}{l_r}, \quad (32)$$

$$l_r = \frac{h_r \cdot \cotg \mu}{\Delta}. \quad (33)$$

The resulting displacement p in point P(ξ, η) is then determined as the sum of all (1 to q) elementary displacement Δp due to working out all EW (1 to q) with positions indices j, i , which may, according to their depth h_r , participate in the displacement p .

$$p(\xi, \eta) = m.a.z(t) \sum_{r=1}^q \frac{g(k_r)}{4 \sum_{i=1}^{[l_r]} \sum_{j=0}^{\lceil \sqrt{l_r^2 - i^2} \rceil} g\left(\frac{\sqrt{i^2 + j^2}}{[l_r]}\right) + g(0)}. \quad (34)$$

This sum was carried out in the sense of equation (16) modified for three-dimensional integration zone Ω and the dependence of the full effective area Φ on the depth h of the differential working $dq = r dr d\varphi dh$.

$$p(\xi, \eta) = m.a.z(t) \iiint_{\Omega} \frac{r \cdot u(r)}{2\pi \int_0^{h \cdot \cotg \mu} r \cdot u(r) dr} dr d\varphi dh.$$

Symbols $[l_r]$ and $\lceil \sqrt{l_r^2 - i^2} \rceil$ in the equation (34) are used for the designation of integer part of these numbers. The complex sum in the denominator of equation (34) expresses the numerically derived value of the double integral, defined by the denominator of the quoted equation under circumstances expressed by relations (31), (32) and (33). It is further evident, from the equation (34), that for the case of a horizontally deposited seam, i.e., when $h_r = \text{const.}$, the denominator of all added fractions will be constant. The equation (34) will then become a direct numerical expression of equation (16). When designing the denominator of the equation (34) by the symbol J_r , we are able – with respect to definitions (9), (10) and (29) – to derive, for individual components of the resulting spatial displacement

s , v_x , v_y in the point $P(\xi, \eta)$ the following expressions

$$s(\xi, \eta) = m.a.z(t) \sum_{r=1}^q \frac{g(k_r)}{J_r} \cdot \frac{1}{\sqrt{1 + k_r^2 \cot^2 \mu}}, \quad (36)$$

$$v_x(\xi, \eta) = m.a.z(t) \sum_{r=1}^q \frac{g(k_r) \cdot \cos \varphi_r}{J_r} \cdot \frac{k_r \cdot \cot \mu}{\sqrt{1 + k_r^2 \cot^2 \mu}}, \quad (37)$$

$$v_y(\xi, \eta) = m.a.z(t) \sum_{r=1}^q \frac{g(k_r) \cdot \sin \varphi_r}{J_r} \cdot \frac{k_r \cdot \cot \mu}{\sqrt{1 + k_r^2 \cot^2 \mu}}, \quad (38)$$

when

$$\sin \varphi_r = \frac{i}{\sqrt{i^2 + j^2}}, \quad \cos \varphi_r = \frac{j}{\sqrt{i^2 + j^2}}, \quad (39)$$

where i , j are those already mentioned position indices and k_r is the value, derived from them by means of the formula (32), related to a certain r -th EW.

It should be added, in connection with possible choice of the effect function $g(k)$, that the author used this function in the form of

$$g(k) = 1 + \varepsilon \frac{\cos(\pi \cdot k) - 1}{2} \quad (39)$$

for the eligible ε within the closed interval of 0 to 1. For $\varepsilon = 1$, the course of the function (39) approaches the curve, defined by the effect function according to Bayer (see Tab. 1) and for $\varepsilon = 0$, the function becomes constant, which agree with the concept of the effect function according to Čechura. Thus, the introduction of the parameter ε enables the function (39) to be controlled continuously and this possibility to be used for carrying out various motion prognoses with respect to their mutual comparison or confrontation with results in situ. Fig. 2 illustrates two alternatives of this function, designated as V_1 ($\varepsilon = 1$) and V_2 ($\varepsilon = 0$).

Equations (35), (36) and (37) have an entirely general validity for any shape of spatial working, thus not only for workings in horizontally deposited seams. However, in such a case, such a working must be derived, in agreement with the applied raster network, into a set of cubic EW $\equiv \Delta^3$ and m put equal to Δ in these equations.

In our effort to prove the generality and universality of these equations, the following analysis is applied to workings in dipping seams. The analysis issues from Fig. 5 with following schematic illustrations: vertical section through rocks overlying the seam, dipping by the angle α from the horizontal plane, and geometric relations between the point $Q(x, y, h_r)$, in which the differential working dq has been carried out and the point P , where the displacement effect of this excavation has been determined. Let the system of horizontal coordinates have its origin in the point P and let its axis x lie within the section plane, which should be, in the same time, also the main vertical of the seam.

Differential displacement dp of the point P as consequence of the differential working dq , can be expressed, according to the equation (1) by relation

$$dp = \kappa \cdot f(x, y) dq = \kappa \cdot g(k) dq, \quad (40)$$

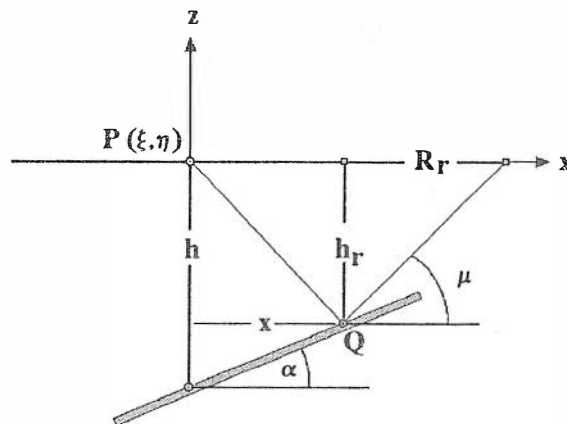


FIG. 5. Effect of a differential working in an inclined seam

in which, under the given circumstances and due to the already mentioned property of the function $g(k)$ as the median curve of the surface $f(x, y)$

$$k = \frac{\sqrt{x^2 + y^2}}{R_r}, \quad (41)$$

when

$$R_r = h_r \cdot \cotg \mu \quad (42)$$

and

$$h_r = h - x \cdot \tg \alpha. \quad (43)$$

R_r is the radius of the circle with centre in the point P, which delimits the horizontal area, beyond which is the effect of all differential workings, lying in the depth h_r , already lower or equal to the value c_0 of the effect function $c = g(k)$ for $k = 1$

$$c_0 = k(1). \quad (44)$$

Thus, this consideration does not again assume the variability of the critical angle with respect to the seam dip, i.e. to the angle, which includes the connecting line \overline{PQ} with the place of the mentioned main vertical. The function $f(x, y)$ defines, within the horizontal plane of the point P, the distribution of effects of all differential workings, which are able to affect the displacement of this point. This distribution is usually expressed graphically by means of contour lines of the same effects, which are, in the case of a horizontally deposited seam, circles with a common centre in the point P. When looking for a certain contour line of the value c , it must hold, for a dipping seam

$$f(x, y) = c, \quad (45)$$

with consideration of relations (42) and (43). For all functions from Tab. 1 or functions of similar shapes including the effect function (39), the equation (45) can

be transformed into

$$\frac{x^2 + y^2}{(h - x \cdot \operatorname{tg} \alpha)^2} = E, \quad (46)$$

and, by its comparison with the canonical ellipse equation

$$\left(\frac{x - m}{a}\right)^2 + \left(\frac{y}{b}\right)^2 = 1,$$

to derive

$$a = \frac{h \cdot \sqrt{E}}{J}, \quad (47)$$

$$b = h \cdot \sqrt{E}, \quad (48)$$

$$m = -\frac{E \cdot h \cdot \operatorname{tg} \alpha}{J^2}, \quad (49)$$

where

$$J = \sqrt{1 - E \cdot \operatorname{tg}^2 \alpha}. \quad (50)$$

The quantity E results from the concrete form of the function $g(k)$. This quantity is quoted in the last column for all functions from the Table 1. Thus, for the effect function (39), this quantity is defined by the expression

$$E = \left(\frac{\arccos \left(\frac{2(c-1)}{\varepsilon} + 1 \right)}{\pi} \right)^2. \quad (51)$$

It is evident, from equations (46) to (49) that ellipses defined by these functions are different size, they have not any common centre, and that for $c = 1$, an ellipse of zero dimension with centre in point P, and for $c = c_0$, the ellipse delimiting the overall area of effects in the neighbourhood of the point P (i.e. the horizontal projection of the full effective area), are formed. It is also evident, from these equations, that both the dimensions and shape of this full effective area, are identical with dimensions and shape of the full effective area, derived for a constant critical angle by some of the known methods of the theory of undermining.

The above mentioned assumption of invariability of the critical angle was introduced only for simplification of reasoning. It is possible to introduce very simply, into the computer forms of equations (35), (36) and (37), an arbitrary functional dependence $\mu = f(i, j)$.

5. ALGORITHM AND SOFTWARE OF AUTOMATED COMPUTING OF MOTION CHARACTERISTICS OF THE UNDERMINED SURFACE OF THE MINE MAYRAU

Algorithms of both the author's software and other previously mentioned softwares have a common goal in the derivation of digital models (DM) of the above-mentioned motion characteristics within the surface extent of the undermined territory studied.

These DM are always of the raster type, used by the author. All motion characteristics are thus determined in each nodal point of the regular square or rectangular network, which involves the entire undermined territory or its selected part with regard to the assumed extent of motion effects, resulting from the known global value of the critical angle for the given mine district. Although this is not a necessary condition, this area of interest is usually chosen in the form of rectangle within the extent of $m \times n$ nodal points. The square network whose elementary side has the length Δ , divides the planned mining area into 1 to q elementary workings EW with dimensions of $m \cdot \Delta^2$ in the case of exploitation of seam with m thickness, and Δ^3 in the case of entirely irregular shapes of workings (chambers, stopes, cavities, etc.).

The basic goal of the first part of automated computing is the derivation of DM of three fundamental motion characteristics, defined by equations (35), (36) and (37), which are contained in three disk sets Fs , Fx , Fy :

- Fs – DM of subsidence,
- Fx – DM of horizontal displacement in the X axis,
- Fy – DM of horizontal displacement in the Y axis.

The organization of the 1st part of computing can be expressed by the algorithm, schematically presented in Fig. 6. The case is of a very simple algorithm in the form of a so-called triple loop. Symbols δs , δv_x , δv_y , which are contained in the middle block of the diagram, represent partial motion contributions of the point $P(\xi, \eta)$ of a certain r -th EW in displacement components. These contributions will obviously not equal to zero only when this EW will lie within the effective area of point P , as demonstrated by Fig. 4.

Sets Fs , Fx and Fy can be considered primary, because they are used as derivation basis for further DM, representing the remaining known motion characteristics of the undermined territory. This applies to:

- Fxy – DM of absolute values of horizontal displacements,
- FDx – DM of dips in the X axis,
- FDy – DM of dips in the Y axis,
- FD – DM of absolute values of dips (mm/m),
- FHx – DM of relative changes of absolute values of horizontal displacements in the X axis,
- FHy – DM of relative changes of absolute values of horizontal displacements in the Y axis,
- FH – DM of relative changes of vertical components of displacements (mm/m),
- Fa – DM of directions of absolute values of horizontal displacements,
- Fr – DM of radii of curvature of the subsidence basin.

All these derived sets are formed on the basis of convolutional filtering of primary sets. This filtering consists of the determination of a certain i, j -th element of DM, those derived elements of the primary DM, which are defined by the position of this (so-called central) i, j -th element. The matters is always of $P(1)$ to $P(9)$ elements, whose position indices against the central point are illustrated by Fig. 7. When designating $O(i, j)$ a certain element of the derived DM, the convolution result can

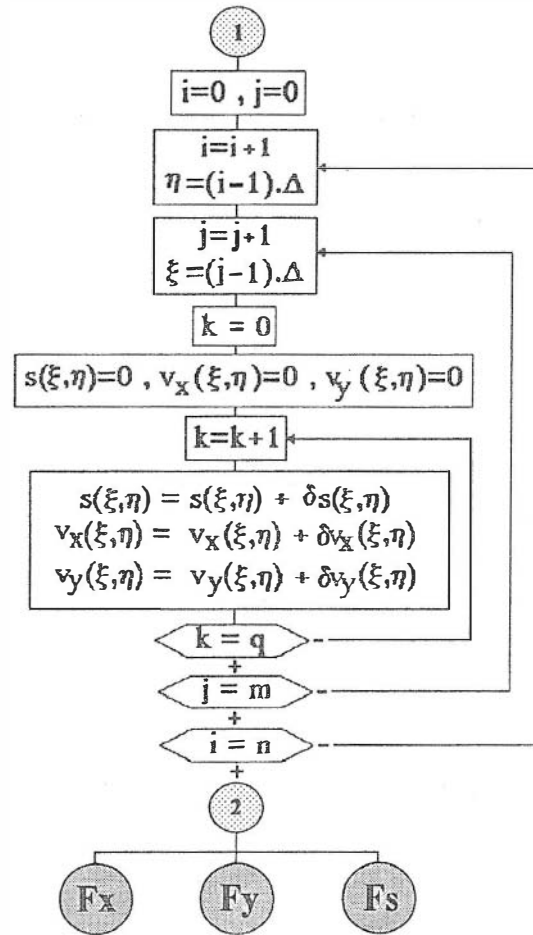


FIG. 6. Block diagram of the first part of algorithm

be expressed by the equation

$$O(i, j) = \sum_{k=1}^9 \varphi(P(k)), \quad (52)$$

where symbol φ expresses the analytical form of this convolution, taking place above 1st to 9th element of the primary DM, assuming that all of the 9 elements need not take part in the convolution at the same time. In the sense of this statement, the above-mentioned derived DM would be formulated as follows:

$$Fxy(i, j) = \sqrt{Fx(i, j)^2 + Fy(i, j)^2}, \quad (53)$$

$$FDx(i, j) = \frac{1}{6\Delta} \sum_{k=i-1}^{i+1} (Fs(k, j+1) - Fs(k, j-1)), \quad (54)$$

$$FDy(i, j) = \frac{1}{6\Delta} \sum_{k=j-1}^{j+1} (Fs(i+1, k) - Fs(i-1, k)), \quad (55)$$

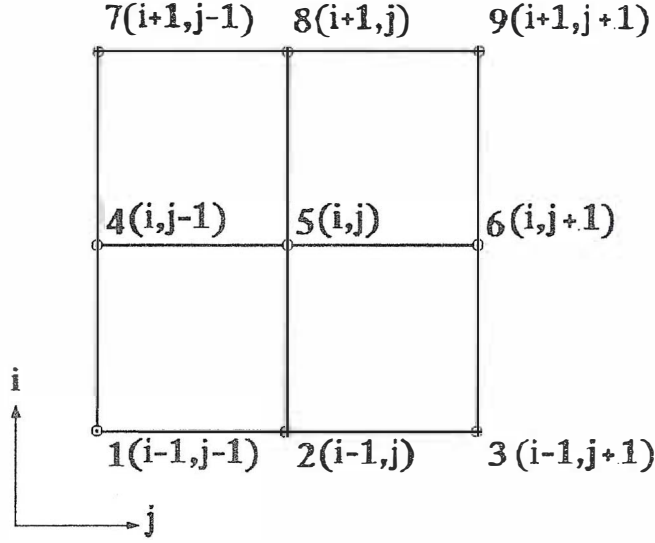


FIG. 7. Position indices of elements of the convolution filter

$$FD(i, j) = \sqrt{FDx(i, j)^2 + FDy(i, j)^2}, \quad (56)$$

$$FHx(i, j) = \frac{1}{6\Delta} \sum_{k=i-1}^{i+1} (Fxy(k, j+1) - Fxy(k, j-1)), \quad (57)$$

$$FHy(i, j) = \frac{1}{6\Delta} \sum_{k=j-1}^{j+1} (Fxy(i+1, k) - Fxy(i-1, k)), \quad (58)$$

$$FH(i, j) = \sqrt{FHx(i, j)^2 + FHy(i, j)^2}, \quad (59)$$

$$Fa(i, j) = \arctg \left(\frac{Fy(i, j)}{Fx(i, j)} \right), \quad (60)$$

$$Fr(i, j) = \frac{1 + FDx(i, j)^2 + FDy(i, j)^2}{1/3 \sqrt{Q_1 - Q_2}}, \quad (61)$$

$$Q_1 = \sum_{k=i-1}^{i+1} (FDx(k, j+1) - FDx(k, j-1)) \times \sum_{k=j-1}^{j+1} (FDy(i+1, k) - FDy(i-1, k)) \quad (62)$$

$$Q_2 = \sum_{k=j-1}^{j+1} (FDx(i+1, k) - FDx(i-1, k)) \times \sum_{k=i-1}^{i+1} (FDy(k, i+1) - FDy(k, i-1)) \quad (63)$$

While the formulation equations (53) to (60) does not require any additional comment, the expression (61) gives the average radius of curvature, derived on the basis of definition of the so-called Gauss' curvature [Rektorys 1968].

It is evident, from the quoted formulations, that DM derived according to equations (54) to (59), will be defined within the range of $(n - 2) \cdot (m - 2)$ and DM according to equation (61) only within the range of $(n - 3) \cdot (m - 3)$ nodal points of the raster network. At an adequate sufficiently dense raster is such a marginal reduction obviously negligible.

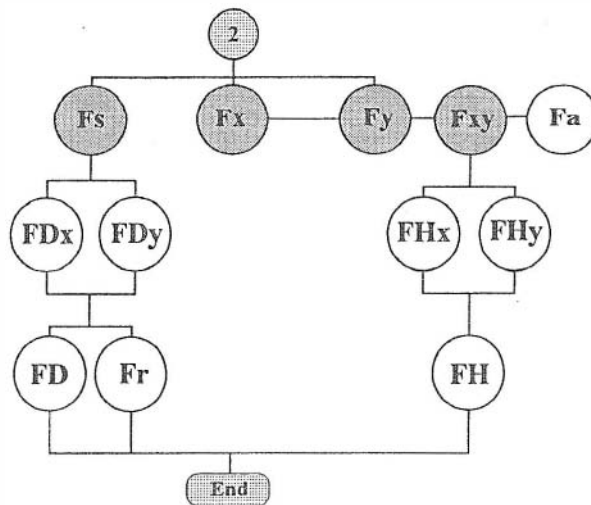


FIG. 8. Block diagram of the second part of algorithm

Fig. 8 explains the formation of these derived DM and represents the block diagram of the 2nd part of the general algorithm, used by the author for the preparation of PC software. The practical application of this software profits of its several important properties and possibilities:

- The effect function chosen by the author in the form (39) can be arbitrarily modified by means of the parameter ε , thus enabling numerical experiments to be carried out for the purpose of confrontation of computed prognoses of undermining effects with in-situ measurements or predictions of another character.
- The empirically defined time function $z(t)$ from the relation (8) is assumed.
- It is assumed that the planned stopes form temporally, dimensionally and typically rounded-off units, so-called boxes. Each box is defined by its contour, which is a closed spatial polygon, defined by breaking points of the box, ending time of exploitation, average seam thickness, assumed exploitation coefficient, and the critical angle of effects.
- Maximum extent of the surface area, where the prognosis is carried out, depends on the choice of the side length of the elementary raster and the maximally allowable number of 40 000 nodal points of this raster.
- In one's endeavour to reduce the time requirements of computing while preserving a more detailed distribution of boxes into EW, it is possible to "dilute" the

density of the surface raster to the half in relation to the original raster density for boxes.

- With the actual software version, the creation of only the following DM is allowed: $F_s, F_x, F_y, F_{xy}, F_{Dx}, F_{Dy}, F_D, F_{Hx}, F_{Hy}, F_H$ and F_a .
- The prognosis can be carried out for an arbitrary depth horizon. This property of the program can be used, to advantage, for determination predictions of a mine shaft.
- An arbitrary DM can be displayed, after ending the program course, by means of the already mentioned author's software, developed for graphical representation of raster-type DM [Vencovský 1989]. As "representation", both the PC-screen display and the formation of a set in the language HPGL are meant, as well as its later plotter-processing. The illustration can be chosen in three various modifications: in the form of contour line plans, coloured hypsometric plans and in the form of "three-dimensional" views. It should be added that the documentation of the hypsometric plans is possible only through a hard copy of the screen display by using a colour printer.

6. RESULTS OF COMPUTER PREDICTION OF SURFACE MOTIONS FOR THE PLANNED EXPLOITATION WITHIN THE SHAFT PILLAR OF THE MAYRAU MINE

Following the requirements of the mine management, these prognoses were made for the planned condition of exploitation at the end of each calendar year, starting by 1993 and ending by the year 2000. All prognoses concerned always the same rectangular territory of dimensions 1100×950 m, the effect of the planned exploitation being not expected beyond this limit, due to the accepted value of critical angle $\mu = 65^\circ$. The overall arrangement of exploited boxes has the form of a horseshoe, situated approximately in the centre of territory and lying at the average depth of 545 m below surface. Prognoses were made in a square-formed network with the side of 10 m, thus for the total number of 10 656 nodal points of this network ($m = 111, n = 96$). However, within the area of workings, this network has been condensed twice, so that horizontal dimension of each EW were 5×5 m, which involved that, for the final condition of exploitation in the year 2000, the total number of EW $q = 4810$. All these prognoses were made for the effect function of the form (39), where $\varepsilon = 1$. They were saved, at the end of 1993, in the chief-surveyor's office of Kladno mines. Prognoses concerned four motion characteristics F_s, F_{xy}, F_D and F_H and they are illustrated in Fig. 9.

At the beginning of 1994, the Modelling laboratory of IRSM constructed the already mentioned equivalent exploitation model of the shaft pillar of the mine Mayrau, aimed at the derivation of such prognoses by a physical method. We had therefore the occasion to compare mutually these both entirely different methods as to their results and to derive new information for rendering computer prognoses more precise, especially with regard to the actual progress of exploitation. A series of alternative computer prognoses with modified the effect functions and the values of the critical angles has been prepared to this purpose. However, these prognoses did not issue from original exploitation parameters for individual boxes, indicated

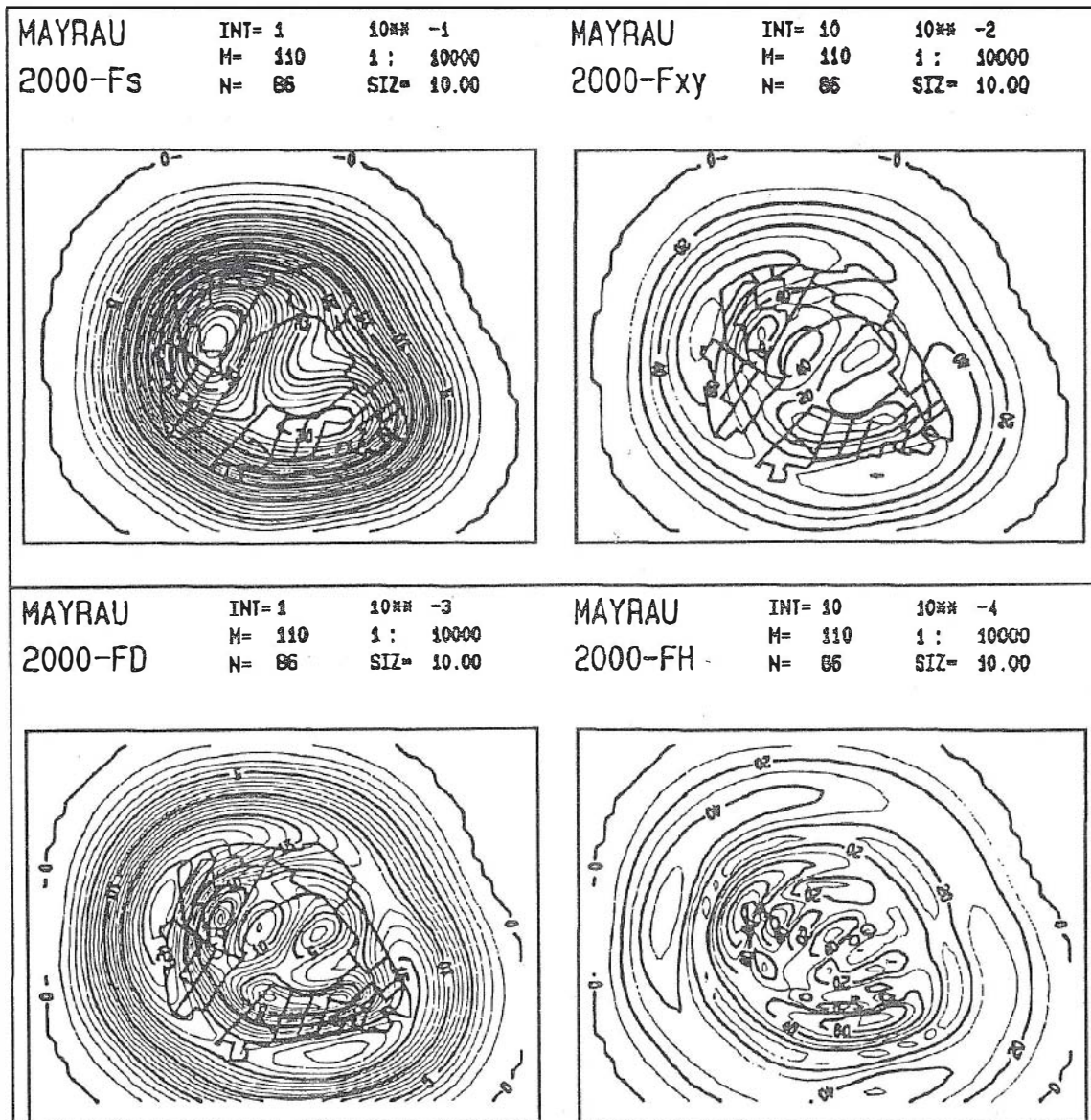


FIG. 9. Graphic form of computer prognoses for the mine Mayrau

by the mine management, but from those of simulated exploitation in the physical model. These parameters – seam thickness and coefficient of exploitation – differed namely sometimes, due to not always perfectly functioning modelling technologies, from the assumed original parameters. The case is therefore of computer-based prognoses of motion characteristics of this very physical model, which enables their direct qualitative and quantitative confrontation with prognoses of physical origin to be carried out.

7. PROGNOSSES OF SURFACE MOTIONS ON THE MAYRAU
MINE, CARRIED OUT BY MEANS OF A PHYSICAL MODEL AND
THEIR COMPARISON WITH COMPUTER-BASED PROGNOSSES

General information about this model have been revealed in the introductory chapter of the book published in [Skořepová, Filip 1994]. It should be added that the surface of the physical model was also derived in the form of digital model prognoses, it has been rendered by the surface of the physical model was rendered and graphical comparisons of two DM of a computer.

The rendered spatial displacement of points defined on the surface of the physical model enabled by the author's software developed in [Skořepová, Filip 1992], for the formation of raster DM of a surface by a general three-dimensional point field. In the formation of the raster DM, a position point field $(X, Y, \Delta X)$, $(X, Y, \Delta Y)$, $(X, Y, \Delta Z)$, from which three digital models Sx , Sy , Sz are formed, called "multiquadric interpolation" [Hardy 1971], is used. From the physical model surface along the individual axes Fx , Fy , Fz , under the given conditions, the digital models Fx , Fy , Fz are derived, and the digital models Sx , Sy , Sz , enabling thus

their comparison was the determination of mean value elements with identical position in each pair of them, $Fy-Sy$, $Fz-Sz$, as well as maximum and minimum values. Obviously, a comparison of the quoted pairs of digital models is only general, because Sx , Sy , Sz models are based on the motion phenomena on the surface of the physical model and with theoretical assumptions, on which they are based. Nevertheless, such comparison may induce the determination of the inherent dissimilarity or affinity of real and theoretical models.

The comparison (Tab. 2 and 3) has been carried out for all three digital models represented by measurements (1020, 1030, 1050) and theoretical models (critical angle $(60^\circ, 65^\circ)$ and effect functions $(V = \text{function (39) for } \varepsilon = 0.10, 0.20, 0.30)$ (Bals, KN = Knothe).

The investigation were then completed, for each state of the physical model, by the determination of the relation (Tab. 4)

$$q_o = \frac{O_p}{O_m} \quad (64)$$

of the volume O_p of the subsidence basin, obtained from DM of the computer prognosis of subsidence and volume O_m , determined from DM of vertical components

TABLE 2.

$\mu = 60^\circ$						
state	function	a_x	m_x	min	max	max - min
1020	V	0.016	0.060	-0.171	0.240	0.411
	BS	0.016	0.067	-0.218	0.316	0.534
	KN	0.016	0.070	-0.250	0.317	0.567
1030	V	0.205	0.208	-0.082	0.681	0.763
	BS	0.205	0.208	-0.115	0.644	0.759
	KN	0.205	0.217	-0.217	0.766	0.983
1050	V	0.012	0.114	-0.348	0.465	0.813
	BS	0.012	0.113	-0.326	0.484	0.810
	KN	0.012	0.138	-0.532	0.571	1.003
state	function	a_y	m_y	min	max	max - min
1020	V	-0.055	0.171	-0.917	0.625	1.542
	BS	-0.057	0.173	-0.917	0.625	1.542
	KV	-0.053	0.178	-0.917	0.625	1.542
1030	V	-0.280	0.302	-1.046	0.318	1.364
	BS	-0.282	0.299	-1.050	0.290	1.340
	KN	-0.277	0.314	-1.035	0.490	1.525
1050	V	-0.334	0.366	-1.050	0.565	1.615
	BS	-0.339	0.361	-1.055	0.440	1.495
	KN	-0.329	0.377	-1.057	0.728	1.885
state	function	a_z	m_z	min	max	max - min
1020	V	0.190	0.208	-0.243	0.702	0.945
	BS	0.187	0.204	-0.243	0.802	1.046
	KN	0.193	0.227	-0.309	1.162	1.471
1030	V	0.102	0.185	-0.322	0.705	1.027
	BS	0.098	0.180	-0.335	0.862	1.197
	KN	0.108	0.235	-0.368	0.959	1.327
1050	V	0.083	0.209	-0.502	0.840	1.342
	BS	0.077	0.190	-0.502	0.720	1.222
	KN	0.092	0.295	-0.527	1.027	1.554

of measured displacements. This ratio illustrates, whether a certain loosening of the modelling material took place during the model experiment, or not.

Following information becomes evident from Tables 2, 3 and 4:

1. Values of parameters m_x , m_y , m_z are lower, when the critical angle of 60° has been introduced into computer prognoses, thus not the angle 65° , which was assumed as one among determining properties of the physical model's equivalent material. It may thus be assumed that the modelling material had properties somewhat different from those assumed.
2. Values of all of these parameters are also lower, if the function according to Bals

TABLE 3.

$\mu = 65^\circ$						
state	function	a_x	m_x	min	max	max - min
1020	V	0.016	0.079	-0.320	0.387	0.707
	BS	0.016	0.084	-0.344	0.381	0.725
	KN	0.016	0.088	-0.414	0.421	0.835
1030	V	0.205	0.216	-0.251	0.764	1.015
	BS	0.205	0.210	-0.136	0.743	0.876
	KN	0.205	0.228	-0.438	0.894	1.332
1050	V	0.012	0.122	-0.565	0.510	1.075
	BS	0.012	0.111	-0.449	0.462	0.911
	KN	0.012	0.157	-0.771	0.641	1.412
state	function	a_y	m_y	min	max	max - min
1020	V	-0.053	0.184	-0.917	0.625	1.542
	BS	-0.053	0.184	-0.917	0.625	1.542
	KV	-0.052	0.192	-0.917	0.625	1.542
1030	V	-0.277	0.308	-1.002	0.482	1.484
	BS	-0.278	0.299	-1.002	0.407	1.409
	KN	-0.276	0.314	-1.002	0.667	1.669
1050	V	-0.330	0.369	-1.042	0.722	1.764
	BS	-0.339	0.359	-1.043	0.632	1.675
	KN	-0.326	0.387	-1.151	0.857	2.008
state	function	a_z	m_z	min	max	max - min
1020	V	0.194	0.228	-0.325	1.230	1.555
	BS	0.193	0.222	-0.307	0.858	1.165
	KN	0.194	0.250	-0.396	1.927	2.323
1030	V	0.108	0.238	-0.378	0.989	1.367
	BS	0.107	0.214	-0.363	1.096	1.459
	KN	0.109	0.290	-0.422	1.661	2.083
1050	V	0.092	0.298	-0.542	1.038	1.580
	BS	0.090	0.254	-0.539	1.471	2.010
	KN	0.095	0.382	-0.554	1.667	2.221

TABLE 4.

state of experiment	g_0
1020	2.26
1030	1.18
1050	1.10

or function (39) for $\varepsilon = 0.75$ are chosen for the effect function. The Knothe's function and functions according to Bayer or Sahn do not characterize the motion

phenomena on the surface of a physical model as well as those effect functions, which, according to equation (44) do not take zero values for $k = 1$.

3. The digital model Sy is affected by much higher measuring errors than the remaining two DM. It is in agreement with the photogrammetric method used. In addition to that, this DM implies also a considerable systematic error, whose origin cannot be identified easily. The Sy model has therefore been eliminated from further comparative analyses.
4. Loosening of the model material in dependence of the volume of simulated exploitation takes place. This is proved by the value of ratio for the starting state 1020, where the exploitation has been carried in two spatially isolated smaller faces. Almost half as big volume of the subsidence basin in relation to the material volume extracted from the model, could also be explained by an insufficiently long time interval of photogrammetric measurement since the exploitation moment. It may be stated, for the final states of the physical model (1030 and 1050), that this loosening is already very small and the differences between measured and predicted subsidence are due only to the behaviour physical model, choice of the effect function and choice of the critical angle in computer-based prognoses.

The comparison of graphic representations of the mentioned DM resulted in the derivation of further information.

In Figs. 10, 11, and 12, the contour-line description of DM of measured subsidences and horizontal components of displacements along the X axis are confronted with corresponding contour-line descriptions of DM of computer prognoses, carried out for two modifications of the effect function, i.e. function (39) and Knothe's function. Fig. 10 related to the state of exploitation 1020, Fig. 11 to 1030 and Fig. 12 to the state 1050, which represented the final state of exploitation on the Mayrau mine in the year 2000. All these prognoses are derived for the critical angle of 60° . Basing upon a detailed analysis of motion actions illustrated in these documents, the following information of a more general, but still hypothetical character, may be derived:

5. The depth of the subsidence basin for an incomplete effective area in the physical model is always smaller than the depth resulting from computer-based prognoses, this even at an approximately similar volume of these basin (an exception is the state of exploitation 1020 – see information 4).
6. The depth of the subsidence basin derived by the computer prognosis for an incomplete effective area depends on the choice of the effect function and of the critical angle. Functions 3, 4 and 5 in Tab. 1 produce deeper basin than function of type 1, 2 or (39) (for $\varepsilon < 0.7$). Deepening of the subsidence basin's bottom, while exploiting the same volume of substance, is produced also by those computer prognoses, where a steeper critical angle has been chosen. This can be understood, because the extent of the affected territory on the surface is reduced and the exploited volume remain unchanged.
7. Shapes of the physically modelled subsidence basins can be considerably different from those computer-assessed, namely at the foot of these basins.

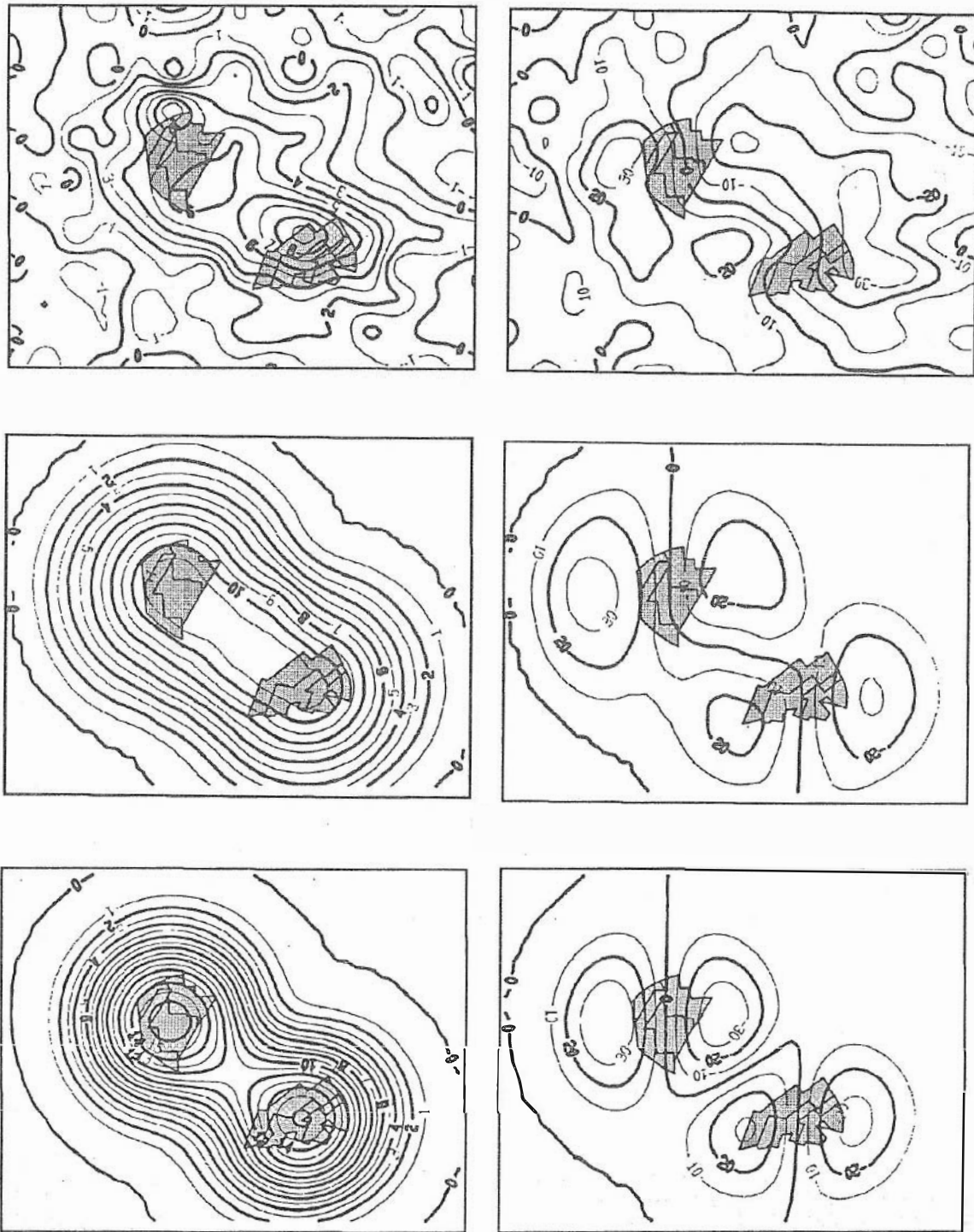


FIG. 10. Comparison of digital models of measured subsidence (10^{-1} m) and horizontal displacements (10^{-2} m) in the x -axis direction (upper pair) with digital models of computer prognoses (intermediate pair for the function (39), the pair below for the Knothe's function). State exploitation 1020.

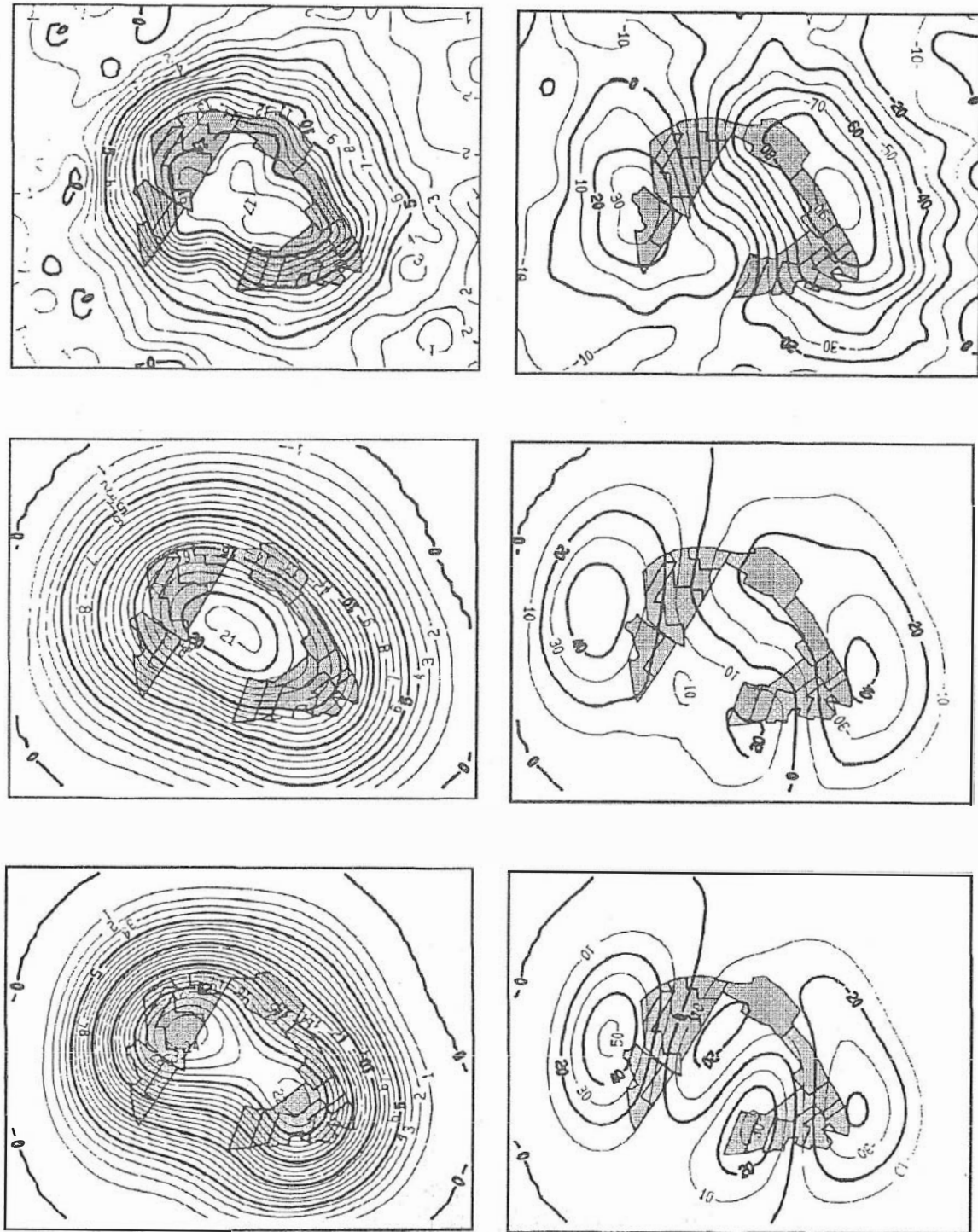


FIG. 11. Comparison of digital models of measured subsidence (10^{-1} m) and horizontal displacements (10^{-2} m) in the x -axis direction (upper pair) with digital models of computer prognoses (intermediate pair for the function (39), the pair below for the Knothe's function). State exploitation 1030.

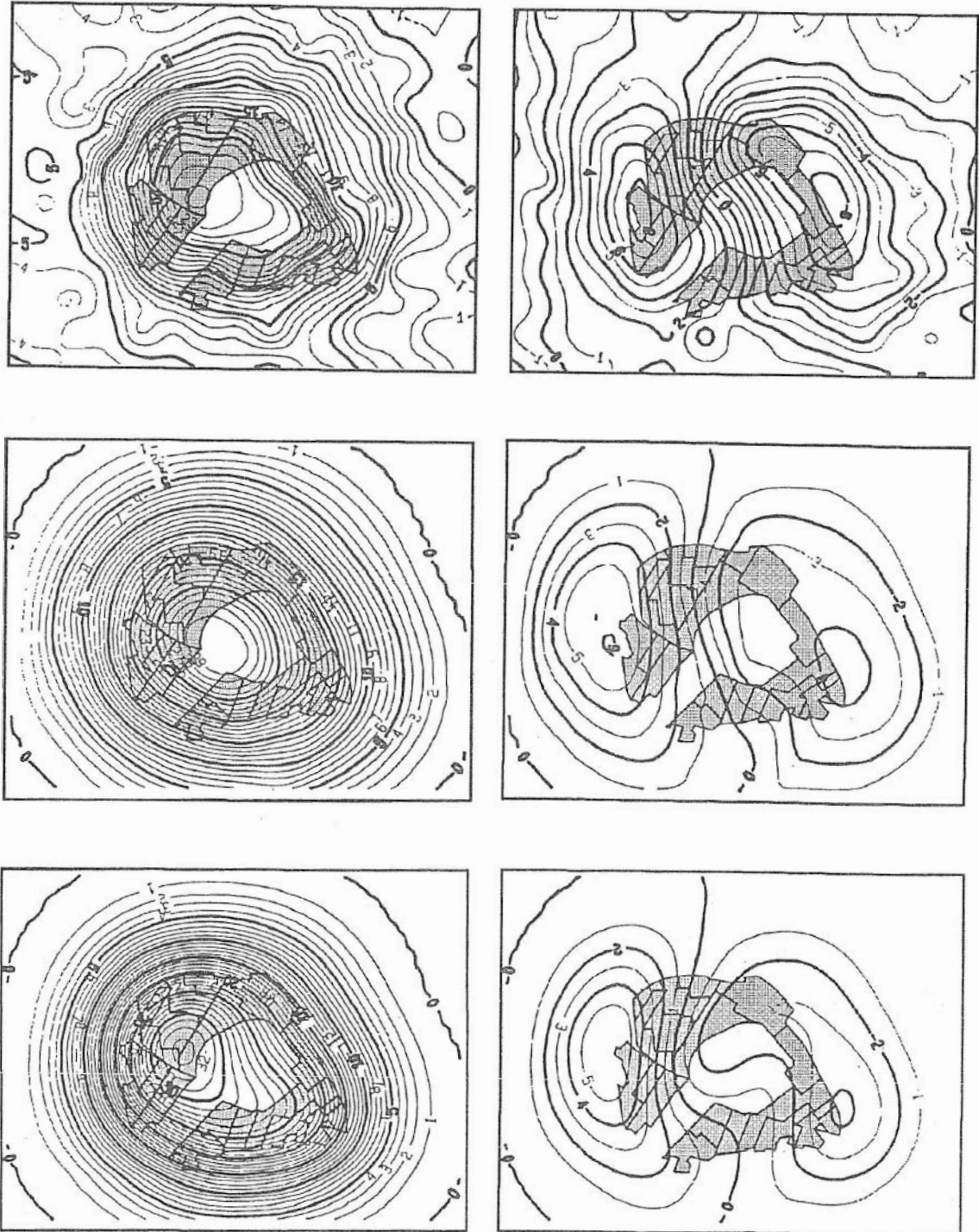


FIG. 12. Comparison of digital models of measured subsidence (10^{-1} m) and horizontal displacements (10^{-1} m) in the x -axis direction (upper pair) with digital models of computer prognoses (intermediate pair for the function (39), the pair below for the Knothe's function). State exploitation 1050.

8. Horizontal displacements of physical character are always bigger than those determined by the computer prognosis, irrespective of the choice of the effect function and the choice of the critical angle. In order to arrive at an at least approximate agreement, it would be necessary to introduce, into these prognoses, another relation than the definition relation (10).
9. The shape of the area for the distribution of horizontal displacements on the surface of a physical model may considerably differ from the respective area, assessed by computer prognosis. Effect function 1, 2 from Tab.1 produce less wavy shapes of the above-mentioned area, being rather more similar to those of the physical origin.

8. CONCLUSIONS

Prediction of motion phenomena on the surface of an undermined territory has been an important information source for both the evaluation and prevention of undermining damage on the surface and in superficial structures. Until now, these prognoses have been carried out only on the basis of theoretical considerations of analytical character, from which the corresponding numerical and actually already fully automated computing procedures have been derived.

Mechano-physical prognoses of the kind have not yet been carried out, neither in our country nor abroad. Results of the motion analysis of the surface of a physical model, carried out in IRSM for the explanation of exploitation consequences within the shaft pillar of the Mayrau mine, may therefore be considered unique. Compared with theoretical considerations, these results should give an account of real deformation of the rock mass due to mining activities. Nevertheless, we have to assume that their quality corresponds with hitherto accumulated, really only sporadic experience with physical models of this kind, so their value should be considered only informative. This fact is affected also by some (today already known) circumstances, connected with the construction technology of the model, which complicated the procedure of comparison with computer-based methods and rendered the modelling of a rather articulated terrain relief on a physical model quite difficult, when, for computer prognoses, a planar surface was taken in account, the volume of the exploited seam shrank due to inadequate function of the modelling equipment, one of modelling stand walls was released during the experiment, etc. However, we may assume that our results are highly valuable and will probably be applied, in the future, in the research of prognoses of effects connected with undermining.

The results of these heterogeneous prognoses and their mutual comparison cannot be used for the preference of the one or the other prognostical methods as to their higher credibility, because we still lack some survey results, which would describe real motion phenomena on the surface of the mine area involved. Today, we can only look for some advantages or drawbacks of these both methods, which could be important for their future development.

Prognoses obtained by means of physical models have the advantage in fact that their rock medium is not defined in a mathematical way, which must be considered,

within the given connection, always a very approximate one. The physical model's equivalent material and the model itself are always constructed with the ambition to involve, in the structure, all accessible geological and mechano-physical information about the original rock massif, thus to be able to assume the qualitative and quantitative affinity of rock-deforming processes, the modelled and the real ones. However, this advantage of physical prognoses is discriminated by several circumstances. First, the above-mentioned assumption cannot be checked to prove, whether the modelled similarity is really successful, then the construction of a physical model is usually lengthy and expensive and finally, it is necessary to construct separate models for alternative changes of physical and geotechnical input parameters. It should also be added, to these discriminating circumstances, the fact that the scale of the physical model must be chosen with regard to real space possibilities of modelling laboratories. Usually, the optimum choice of the scale is inconsistent with these possibilities. This was also the case of the studied model, whose scale 1:750 proved to be too small to attain the required precision in the derivation of predicted displacements of the model surface by the used measurement method.

Theoretical computer prognoses have, on the other hand, several undoubted advantages. Most important is their economical and time-requiring feasibility as well as the acquirement of large number of alternative prognoses for the alternation of both the input parameters and eventual changes of some theoretical assumptions. Their only but very important drawback is the mentioned and always necessary simplification of the problem in order to render it definable analytically. However, this simplification can sometimes involve the inadequacy of computer-based methods as suitable tools for the solution of the problem requiring their further and time-wasting improvements.

REFERENCES

- Neset K. (1984), *Effects of Undermining*, SNTL. (in Czech)
- Skořepová J. and Filip D. (1994), *Prediction of settlement during the exploitation of a shaft pillar*, Proc. XIth Danubia-Adria Symposium on experimental methods in solid mechanics, Baden (Austria), pp. 93-94.
- Lucák O. (1969), *Manifestation of undermining effects on the surface of Kladno coal district*, Dissertation, Mining Inst. ČSAV. (in Czech)
- Kadainka V. (1937), *Character of surface and effects of exploitation in the Kladno coal district*, Hornický věstník. (in Czech)
- Vencovský M. (1989), *Methods of measurement and graphical illustration of deformations of physical rock mass models. D. Dissertation*, Inst. Geol. Geotechn. ČSAV, Praha, 69-74. (in Czech)
- Vencovský M. (1992), *Deformation analysis of physical rock mass models*, Acta Montana A1(87), 69-74.
- Havlík F. (1967), *Computing the point subsidence on the surface according to Niederhofer on ZUSE Z-23 computer*, Rudy 12, 405-408. (in Czech)
- Hradil J. (1969), *Computing the subsidence of surface points on a medium computer*, Uhlí 12, 450-453. (in Czech)
- Čimbura V., Hynčicová J. (1994), *Practical utilization of undermining effects calculation in IMG E Comp. for the needs of OKD*, Proc. IXth Congress ISM, Praha, pp. 73-77.
- Murysová R., Vočyán J. (1994), *Die Rechnerunterstützung bei der Ermittlung der Einflüsse der Unterbauung und deren Einwirkungen auf die Oberfläche*, Proc. IXth Congress ISM, Praha,

pp. 448–453.

Neubert K. (1958), *Beitrag zur Vorausberechnung von Bodenbewegungen*, Markscheidewesen, vol. A86, Freiburger Forschungshefte, pp. 68–92.

Rektorys J. (1968), *Review of Applied Mathematics*, SNTL, Praha. (in Czech)

Hardy R.L. (1971), *Multiquadratic equation of topography and other irregular surfaces*, J. Geophys Res. **76**, 1905–1915.